Electroproduction of π^+ from ^{10}B and its relation to electron scattering

B. W. Zulkoskey, R. M. Sealock, H. S. Caplan, and J. C. Bergstrom
Saskatchewan Accelerator Laboratory, University of Saskatchewan, Saskatoon S7N 0W0 Canada
(Received 30 March 1982)

The electroproduction of 12.3 ± 0.7 MeV positive pions from ^{10}B, leading to low-lying states in ^{10}Be, has been measured in the angular range $\theta_\pi=30°-140°$ for incident electron energies $E_e=158.5-165.0$ MeV. The unique character of $M3$ transitions in the p shell permits a direct comparison of $d^2\sigma/dE_\pi d\Omega_\pi$ with the analog electron scattering form factors in ^{10}B, assuming the strong π-nucleus interaction can be neglected. For the two lowest $T=1$ states, the (e,π^+) angular distributions agree with the $M3$ form factors. The convective term in the $M1$ form factor for the third $T=1$ state is deduced from a comparison of the (e,π^+) and (e,e') data and is in good agreement with recent radiative pion capture results. The photoproduction cross section leading to the ^{10}Be ground state is estimated.

[NUCLEAR REACTIONS ^{10}B$(e,\pi^+)e'$ ^{10}Be; $E_e=158.5-165.0$ MeV; $E_\pi=12.3$ MeV; measured $\sigma(E_\pi,\theta_\pi)$; $\theta_\pi=30°-140°$; compare to electron scattering, radiative pion capture, and photoproduction.]

I. INTRODUCTION

The photoproduction or electroproduction of pions in the energy range $E_\pi \lesssim 20$ MeV, leading to specific nuclear states, offers a method for probing the pion-nucleus interaction in a region bridging elastic pion scattering and conventional radiative pion capture (RPC). In order to study the final-state interaction, one clearly must minimize any uncertainties in the nuclear structure which could effect the $(\gamma,\pi^\pm)$ or $(e,\pi^\pm)$ cross sections. In this paper we describe possible candidates for transitions where one could have a measure of confidence in these structural effects.

Often in the past such structural information has been provided by the electron scattering form factors for the corresponding analog states in the target nucleus. The problem is that, in general, both the spin (i.e., magnetization) currents and the convection currents contribute to the (e,e') transitions, while the $(\gamma,\pi^\pm)$, $(e,\pi^\pm)$, and RPC transitions depend predominantly on the spin densities. Thus, one must rely on some kind of model-dependent analysis of the electron scattering form factors, phenomenological or otherwise, to separate these contributions, or simply ignore the convection terms in the expectation that they are small.

This model dependence can be kept to a minimum in selected cases, such as $M3$ transitions in p-shell nuclei where the convection terms vanish in a $(1p)^n$ model space[1] and only one spin-dependent matrix element participates. Specifically

$$F_{M3}(q)\propto q\,|\,\langle J_f||\vec{\mathrm{M}}_{\lambda\lambda-1}\cdot\vec{\sigma}\tau_z||J_i\rangle\,|_{\lambda=3}\,, \tag{1}$$

where

$$\vec{\mathrm{M}}^{\mu}_{\lambda\lambda'}=j_{\lambda'}(qr)\vec{\mathrm{Y}}^{\mu}_{\lambda\lambda'}(\Omega) \tag{2}$$

and in our notation a sum over nucleons is implied.

The situation is similar for radiative pion capture from $1s$ and $2p$ atomic orbitals in p-shell nuclei. For $M3$ transitions the spin-independent terms vanish for reasons of parity, and if one makes the reasonable assumption that the pionic wave functions inside the nucleus, $R_{nl}(r)$, vary as r^l, then only two matrix elements survive, namely

$$\langle J_f||\vec{\mathrm{M}}_{\lambda\lambda-1}\cdot\vec{\sigma}\tau^-||J_i\rangle$$

and its derivative with respect to q. In other words, except for rotation in isospin space, the same nuclear matrix elements occur in the (e,e') and (π^-,γ) transitions. Therefore the relative magnitudes of the $M3$ form factors evaluated at the momentum transfer appropriate to RPC should equal the relative magnitudes of the RPC branching ratios for the analog states.

This was nicely confirmed[2] in a study of the low-lying $T=1$ states of ^{10}B and ^{10}Be, shown in Fig. 1. The transition to the 1.74 MeV state of ^{10}B is necessarily $M3$, and electron scattering established the $M3$ nature of the 5.17 and 8.89 MeV form factors.[3] At the RPC point ($q\approx0.67$ fm^{-1}) the $M3$

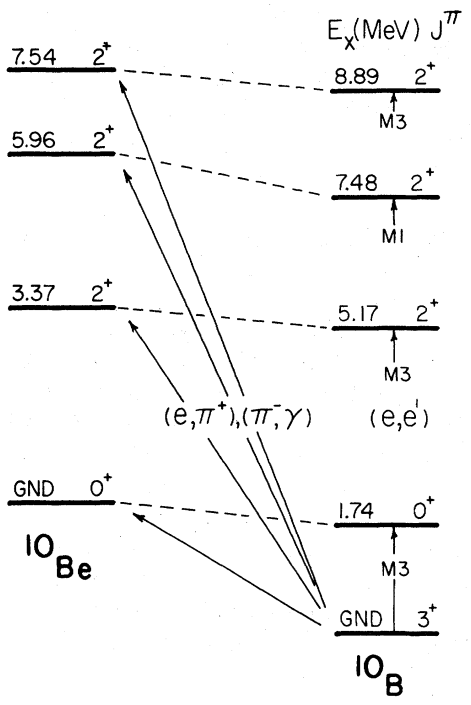

FIG. 1. The low-lying $T=1$ states of ^{10}Be populated by the reactions (e,π^+) (this work) and (π^-,γ) (Ref. 2) on ^{10}B. Also shown are the corresponding analog states in ^{10}B. The transition multipolarities to the 2^+ states in ^{10}B, and the J^π assignment for the 7.48 MeV state, are based on the (e,e') results of Ref. 3.

form factors of ^{10}B give

$$\frac{F_{5.17}{}^2}{F_{1.74}{}^2}=2.30 \text{ and } \frac{F_{8.89}{}^2}{F_{1.74}{}^2}=0.40 ,$$

while for the RPC branching ratios one obtains[2]

$$\frac{R_\gamma(3.37)}{R_\gamma(\text{g.s.})}=2.30\pm0.24$$

and

$$\frac{R_\gamma(7.54)}{R_\gamma(\text{g.s.})}=0.39\pm0.12 .$$

In the present work we have investigated the electroproduction reaction $^{10}\text{B}(e,\pi^+)e'^{10}\text{Be}$ leading to the ground state $(0^+;1)$ of ^{10}Be and the excited states at 3.37 MeV $(2^+;1)$, 5.96 MeV $(2^+;1)$, and 7.54 MeV $(2^+;1)$. The (e,π^+) and RPC operators are similar in structure and the respective reactions share certain features; for example, within the limits of certain simplifying assumptions discussed later, the $M3$ electroproduction cross sections are directly proportional to matrix elements of the type in Eqs. (1) and (2), with the appropriate isospin modification. That is, *the (e,π^+) double differential cross sections are proportional to the analog $M3(e,e')$ form factors* evaluated at the appropriate momentum transfers.

No direct comparison between the (e,e') and (e,π^+) cross sections can be made for the 5.96 MeV state in ^{10}Be (7.48 MeV in ^{10}B). Electron scattering identifies this as an $M1$ excitation, and hence, the convection terms may not be negligible. In fact, combined analysis of the form factor and the RPC rate suggest the spin and convection matrix elements are comparable and interfere destructively.[2] One would therefore expect the experimental (e,π^+) cross section to be somewhat larger than the predictions based on the 7.48 MeV form factor if the convection contributions are ignored.

Our measurements are in accord with this expectation. Furthermore, we show that the $M3$ cross sections are well described by the corresponding electron scattering form factors; hence all three reactions, (e,π^+), (e,e'), and (π^-,γ) are mutually consistent. Finally, we consider the photoreaction $^{10}\text{B}(\gamma,\pi^+)^{10}\text{Be(g.s.)}$ and compare it with recent measurements.

II. EXPERIMENTAL DETAILS AND RESULTS

This experiment was performed at the 250 MeV linear accelerator facility at the University of Saskatchewan. The angular distributions of 12.3 ± 0.7 MeV pions were measured in the range $\theta_\pi=30°-140°$ for incident electron energies of 158.5, 160.3, 162.0, and 165.0 MeV. These energies were chosen so that successive states of interest in ^{10}Be would be populated in association with the production of 12.3 MeV pions. Thus at 158.5 MeV the ground and 3.37 MeV states are accessible, while at an energy of 160.3 MeV, excitation of the 5.96 MeV state becomes possible as well. The 7.54 MeV level is included at 162.0 MeV, and for an incident energy of 165.0 MeV it is possible for ^{10}Be to be excited somewhat above 7.54 MeV. The threshold for given excitation and pion energies depends on the pion angle; for example, at 160.3 MeV the kinematic cutoff for the 5.96 MeV state occurs near $\theta_\pi=80°$.

Pions were detected by a four-telescope array mounted in the focal plane of a 50 cm double-focusing spectrometer, whose deflection is about 127°. The total momentum acceptance of the array

is ±3%. Each telescope was comprised of three silicon surface barrier detectors, the details of which are described in Ref. 4. Aluminum moderators with thicknesses of 2.0–2.8 mm were located in front of the telescopes to ensure that the 12 MeV pions stopped near the midplane of the third detector.

The targets were fabricated of 96.2% enriched polycrystalline ^{10}B powder confined between beryllium windows, each 4 mg/cm^2 thick. The windows were separated and supported by an aluminum spacer which was split to prevent any pressure differential between the target interior and exterior. The target thicknesses, 60 and 74 mg/cm^2, were determined from the known mass of the boron powder and the target surface area, assuming uniform distribution. No contamination of the spectra by pion production from beryllium or ^{11}B was possible since we operated below their respective thresholds.

Measurements of proton yields were used to check the uniformity of the target. Also each pion run was bracketed by measurements of protons. This technique enabled us to detect changes in density during prolonged exposure to the electron beam. After the experiment these changes were found to be due to local sintering of the boron powder. When a density change occurred the pion run was discarded and a fresh spot on the target was used. The pion yields were then normalized, if necessary, using the proton yield from the new spot. The final errors in the pion cross sections in part reflect the uncertainties in these corrections.

The pion yields were corrected for background, pion decay in flight (nearly 50%), losses due to multiple scattering in the telescopes, and photopion production from bremsstrahlung generated within the target. For the latter we relied on the measurements of Stoler *et al.*[5] modified for the present geometry, resulting in a correction of about 7%. The experimental double differential cross sections were deduced for each detector telescope using the known spectrometer acceptance, detector momentum acceptance, etc. The final results are presented in Table I and Figs. 2–5 as averages over the four telescopes.

III. COMPARISON WITH ELECTRON SCATTERING

We wish to make a qualitative comparison between the (e,π^+) and (e,e') cross sections, and to this end several approximations will be made. We assume the plane-wave forward-peaking approximation[6,7] can be applied to the undetected electron despite the large energy loss. In this limit terms like $\vec{k}(\vec{\sigma}\cdot\vec{k})/\omega_\gamma^2$ which contribute to the so-called longitudinal matrix elements are negligible, as are terms depending on the pion momentum for the pion energies considered here. The electroproduction cross section may then be written

$$\frac{d^2\sigma}{dE_\pi d\Omega_\pi}=\frac{N}{\omega_\gamma}\left[\frac{d\sigma}{d\Omega_\pi}\right]_\gamma, \tag{3}$$

where N is the virtual photon spectrum,[8] ω_γ is the photon energy, and $(d\sigma/d\Omega_\pi)_\gamma$ is the photopion differential cross section involving only the usual $\vec{\sigma}\cdot\vec{\epsilon}_\lambda$ threshold operator.

In evaluating the photopion cross section we ignore the strong pion-nucleus interaction and treat the pion as a plane wave modified by the Gamow factor $C_0(\eta)$ to partly account for Coulomb distortion.[9] The limited accuracy of the present data does not justify a detailed treatment of the strong interaction, whose effects in any case are expected to be minor in comparison with the Coulomb distortion. With these assumptions the differential (γ,π^+) cross section in the impulse approximation and the laboratory frame is given by

TABLE I. Double differential cross sections for the reaction ^{10}B$(e,\pi^+)e'^{10}$Be for pion kinetic energies 12.3±0.7 MeV, as determined in this work. The units are 10^{-36} cm^2/ MeV sr. The incident electron energies are E_e while θ_π represents the observed pion angle in the laboratory frame, with respect to the incident beam.

E_e (MeV) \ θ_π	30°	40°	90°	120°	132°	140°
158.5	1.9±0.9	2.4±0.6	4.8±0.8		4.6±0.8	3.8 ±0.9
160.3	11.3±1.9		6.6±0.9		8.3±1.0	12.1±1.2
162.0	28.0±2.3	22.2±1.5	10.7±0.8	14.1±1.7		13.6±1.3
165.0	44.2±4.6		20.9±1.7			26.6±2.6

$$\left[\frac{d\sigma}{d\Omega_\pi}\right]_\gamma = 2\alpha\left[\frac{f}{m_\pi}\right]^2\left[\frac{p_\pi}{k_\gamma}\right]\left[1+\frac{m_\pi}{2M_n}\right]^{-2}\left[1+\frac{E_\pi}{M_{A'}}\left[1-\frac{k_\gamma}{p_\pi}\cos\theta_\pi\right]\right]^{-1}$$

$$\times\frac{1}{2J_i+1}\sum_{M_iM_f}\tfrac{1}{2}\sum_\lambda C_0{}^2(\eta)\,|\,\langle J_fM_f\,|\,e^{i\vec{q}\cdot\vec{r}}(\vec{\sigma}\cdot\vec{\epsilon}_\lambda)\tau^-\,|\,J_iM_i\rangle\,|^2\,, \tag{4}$$

where m_π, M_n, and $M_{A'}$ are, respectively, the pion, nucleon, and final nuclear masses, $(E_\pi,\vec{p}_\pi)$ are the pion total energy and momentum, $(\omega_\gamma,\vec{k}_\gamma)$ are the photon energy and momentum, and $\vec{q}=\vec{k}_\gamma-\vec{p}_\pi$ is the momentum transferred to the nucleus. We take the π-nucleon coupling constant to be $f^2=0.081$. The isospin-lowering operator is defined by $\tau^-\,|\,p\rangle=|\,n\rangle$ and differs by a factor of $\sqrt{2}$ from the conventional spherical tensor.

The sums in Eq. (4) are performed in the usual manner by expanding the operator in a multipole series and applying the Wigner-Eckart theorem. We chose the quantization axis along $\vec{k}_\gamma$ (i.e., $\vec{k}_\gamma\cdot\vec{\epsilon}_\lambda=0$), and for $M\lambda$ transitions obtain

$$\sum_{M_iM_f}\tfrac{1}{2}\sum_\lambda|\,\langle J_fM_f\,|\,e^{i\vec{q}\cdot\vec{r}}(\vec{\sigma}\cdot\vec{\epsilon}_\lambda)\tau^-\,|\,J_iM_i\rangle\,|^2=\frac{4\pi}{2\lambda+1}\left[\langle J_f||\vec{M}_{\lambda\lambda-1}\cdot\vec{\sigma}\tau^-||J_i\rangle^2\left[\frac{\lambda+1}{2}+\frac{\lambda-1}{4}\sin^2\theta_q\right]\right.$$

$$+\langle J_f||\vec{M}_{\lambda\lambda+1}\cdot\vec{\sigma}\tau^-||J_i\rangle^2\left[\frac{\lambda}{2}+\frac{\lambda+2}{4}\sin^2\theta_q\right]$$

$$-\langle J_f||\vec{M}_{\lambda\lambda-1}\cdot\vec{\sigma}\tau^-||J_i\rangle\langle J_f||\vec{M}_{\lambda\lambda+1}\cdot\vec{\sigma}\tau^-||J_i\rangle$$

$$\left.\times[\lambda(\lambda+1)]^{1/2}(1-\tfrac{3}{2}\sin^2\theta_q)\right]\,, \tag{5}$$

where the multipole operators are defined by Eq. (2), and θ_q is the direction of the recoiling nucleus with respect to $\vec{k}_\gamma$. Finally, we assume that the individual nuclear matrix elements in Eq. (5) can be related to the corresponding electron scattering matrix elements by isospin rotation. Between states of isospin $T_i=0$ and $T_f=1$ we have

$$\langle J_f||Q\tau^-||J_i\rangle^2=\tfrac{1}{2}\langle J_f||Q\tau_z||J_i\rangle^2\,, \tag{6}$$

where Q is the appropriate multipole operator.

In general, the complete expression given by Eq. (5) cannot be related to the $M\lambda$ form factor by isospin rotation since the combination of multipole operators here is not equivalent to that projected by the vector current in an electromagnetic transition. However, for $M\lambda$ transitions of maximum multipolarity within a given configuration space, only the matrix elements of $\vec{M}_{\lambda\lambda-1}\cdot\vec{\sigma}$ are nonvanishing and Eq. (5) is then directly proportional to the square of the analog form factor.

The differential electroproduction cross section for these "stretched" $M\lambda$ transitions is obtained from Eqs. (3)–(6), with the result

$$\frac{d^2\sigma}{dE_\pi d\Omega_\pi}=\tfrac{1}{2}N\alpha\frac{p_\pi}{k_\gamma{}^2}\left[\frac{f}{m_\pi}\right]^2\left[1+\frac{m_\pi}{2M_N}\right]^{-2}C_0{}^2(\eta)\chi(\theta_\pi,\theta_q)Z^2\left[\frac{4M_n}{\mu_p-\mu_n}\right]^2\left[\frac{F_{M\lambda}{}^2(q)}{q^2}\right]\,, \tag{7}$$

where $\mu_{p,n}$ is the nucleon magnetic moment, $F_{M\lambda}(q)$ is the form factor for the analog state, and

$$\chi(\theta_\pi,\theta_q)=\left[1+\frac{\lambda-1}{2(\lambda+1)}\sin^2\theta_q\right]\Big/\left[1+\frac{E_\pi}{M_{A'}}\left[1-\frac{k_\gamma}{p_\pi}\cos\theta_\pi\right]\right]\,. \tag{8}$$

This factor is essentially unity for the present kinematics.

Equation (7) gives the required relation between the $M3$ form factors of ^{10}B and the corresponding (e,π^+) cross sections. The form factors for the 1.74, 5.17, and 8.89 MeV states were obtained from the Helm model fits to the Saskatoon electron scattering data described in Ref. 3, but here we ig-

nore the small $M1$ contributions possibly present for some states at low momentum transfers. Note that we have used these fits merely as an interpolative device and do not rely on the resulting densities for any aspect of the analysis.

We have also included the 7.48 MeV $M1$ form factor in the analysis, ignoring any influence of the convection currents. The angular distributions depend on the ratio $F_{M\lambda}{}^2(q)/q^2$ which is strongly multipole dependent, varying roughly as $q^{2\lambda-2}$ for small momentum transfers. Since q increases with θ_π, the $M1$ cross section should be predominant at the forward pion angles while the higher multipoles should dominate the back-angle cross sections. (This conclusion carries over into more detailed treatments of electroproduction as can be seen, for example, in the work of Nagl and Überall[10] on the $M2$ and $M4$ transitions in ^{12}C.) One may show that, in the limit $\theta_q \to 0$, Eq. (5) is proportional to the purely spin-dependent part of $F_{M1}{}^2(q)$. However, for the present kinematics $\theta_q \lesssim 22°$, and hence, Eq. (7) can only be considered a rough guide to the $M1$ (e,π^+) cross section, even in the absence of convection currents.

The cross sections were calculated for the kinematic conditions appropriate to each detector telescope, and an average over the four telescopes was formed to compare with experiment. The results are shown in Figs. 2–5.

Figure 2 represents the least ambiguous situation

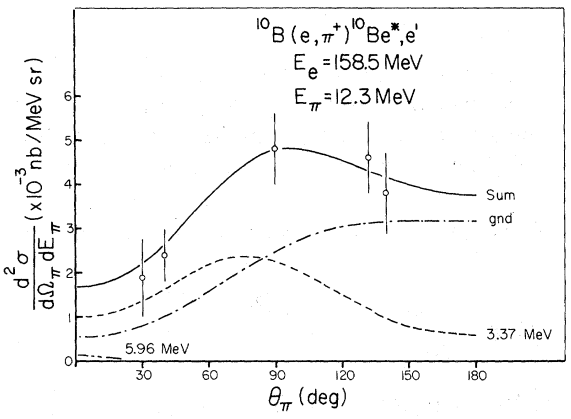

FIG. 2. Double differential cross sections for the (e,π^+) reaction leading to the ground plus first excited states of ^{10}Be, for an incident energy $E_e = 158.5$ MeV and detected pion energies of 12.3 ± 0.7 MeV. The curves are predictions based directly on the experimental $M3$ form factors for the 1.74 MeV (0^+) and 5.17 MeV (2^+) states of ^{10}B as discussed in the text. The gradual decrease in the 3.37 MeV curve is due to the kinematic cutoff for excitation of this state which does not occur simultaneously in all detectors.

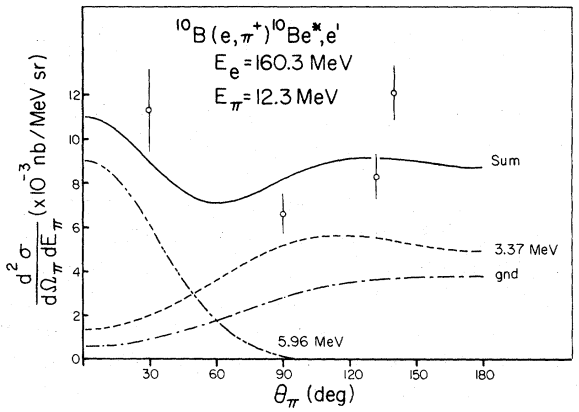

FIG. 3. Same as Fig. 2, but for $E_e = 160.3$ MeV. The threshold for population of the 5.96 MeV state has now been crossed causing an increase in the forward-angle cross section, consistent with the behavior expected for an $M1$ transition.

since only the lowest $M3$ excitations participate. Agreement with experiment is seen to be quite satisfactory, not only in magnitude but also as a function of θ_π. The drop in the 3.37 MeV cross section at large angles is due to the kinematic cutoff which does not affect all telescopes simultaneously.

Figures 3 and 4 show the onset of forward peaking in the experimental cross section caused by the 5.96 MeV $M1$ transition. As expected, the $M3$ cross sections dominate at large θ_π where theory and experiment are still in approximate agreement. The forward-angle discrepancy will be discussed in the next section.

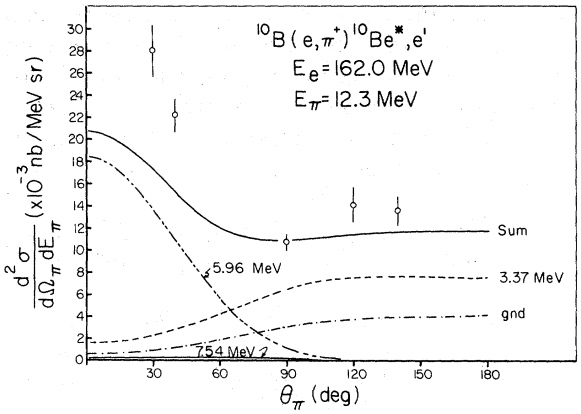

FIG. 4. Same as Fig. 2, but for $E_e = 162.0$ MeV. Excitation of the 7.54 MeV state is now possible. As in Fig. 3, the 5.96 MeV prediction is based directly on the 7.48 MeV $M1$ form factor in ^{10}B. The discrepancy with the forward-angle data is interpreted as a destructive interference between the spin and convection terms in the $M1$ form factor.

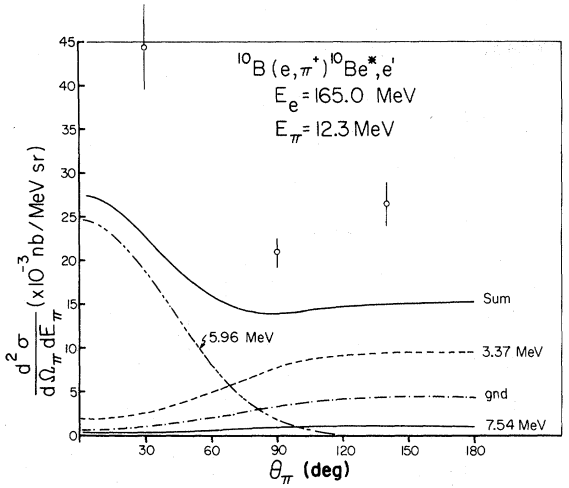

FIG. 5. Same as Fig. 2, but for $E_e = 165.0$ MeV. At this energy it is possible for ^{10}Be to be excited somewhat above 7.54 MeV.

At the highest incident energy (Fig. 5) too many new states become accessible to form any conclusions except that perhaps some forward peaking in the cross section still prevails. The $M3$ contribution from the 7.54 MeV state is weak in all the angular distributions because of the small relative strength of the analog 8.9 MeV form factor in ^{10}B.

IV. DISCUSSION AND CONCLUSION

Angular distributions of 12.3 ± 0.7 MeV pions from the ^{10}B$(e,\pi^+)e'\,^{10}$Be reaction leading to low-lying $T=1$ states in ^{10}Be have been measured for pion angles $\theta_\pi = 30° - 140°$. The ^{10}Be ground and first excited state (3.37 MeV) are populated by $M3$ transitions and in a $(1p)^n$ model space would be in the category of so-called stretched transitions. In such cases the (e,π^+) cross sections are directly proportional to the analog (e,e') form factors, assuming the pions can be treated simply as Coulomb distorted plane waves. Using this relationship, the present double-differential cross sections were shown to be in accord with the experimental form factors of Ansaldo *et al.*[3] within experimental errors of about 20%.

In the Introduction we reviewed the argument presented by Truöl[2] showing agreement between the (e,e') and RPC studies for the lowest analog states in ^{10}B and ^{10}Be. With the present work internal consistency has now been established for all three reactions, (e,e'), (e,π^+), and (π^-,γ), for the two lowest analog states. For comparison, the momentum transfers to the nucleus in the (e,π^+) study are $q \approx 0.53 - 1.02$ fm^{-1} which encompasses the RPC point, $q \approx 0.67$ fm^{-1}.

We now discuss the third analog state $(2^+;1)$ which lies at 5.96 MeV in ^{10}Be. The forward peaking of the experimental (e,π^+) cross section which occurs when population of this state becomes possible is consistent with the $M1$ assignment given by the (e,e') work, but the magnitude of the cross section based directly on the analog form factor is clearly too small. Since the convection contribution has not been removed from the form factor in calculating the (e,π^+) cross sections, this implies that destructive interference is occurring between the spin and convection terms. The same conclusion was reached in the RPC experiments.[2]

Comparison with the RPC deduction can be made more quantitative by assuming, as in Ref. 2, that the operator $\vec{M}^{\mu}_{\lambda\lambda+1}\cdot\vec{\sigma}$ does not contribute significantly to the 7.48 MeV $M1$ form factor of ^{10}B. Then, following the notation of those authors, we have

$$F_{M1}(q) \propto q\,[(\mu_p - \mu_n)R_{01} + L_{01}]\,, \tag{9}$$

where R_{01} is proportional to

$$\langle J_f || \vec{M}_{10}\cdot\vec{\sigma}\tau_z || J_i \rangle$$

and L_{01} is the convection term. In this approximation, Eq. (5) reduces to a single term, independent of θ_q, and the (e,π^+) cross section is then directly proportional to $|R_{01}|^2$. From the forward-angle data in Figs. 3 and 4 and the experimental form factor one obtains

$$\frac{L_{01}}{R_{01}} = -1.05 \pm 0.11\,,$$

to be compared with the RPC result

$$\frac{L_{01}}{R_{01}} = -1.04 \pm 0.14$$

(see Ref. 2). Thus, within the framework of the same model assumptions, the agreement between the (e,e'), (e,π^+), and (π^-,γ) experiments extends to the third analog state in the ^{10}Be-^{10}B systems.

We now consider the photopion reaction leading to the ^{10}Be ground state. It is not possible to reduce the present data directly to the equivalent (γ,π^+) cross sections by Eq. (3), but we can make an estimate of the ground state cross section with the assistance of the electron scattering form factors. The broken curves in Fig. 2 are based on the 1.74 and 5.17 MeV $M3$ form factors of ^{10}B as previously described. The effective (e,π^+) cross section to the 3.37 MeV state of ^{10}Be, but not the ground state, is

suppressed somewhat by the kinematic cutoff as one moves across the focal plane of the spectrometer. From the *ratio* of these curves one can derive the relative contribution of the ground state transition to the total cross section that is nearly independent of the pion distortion, and application of these renormalization factors to the experimental data yields the electropion cross section to the ^{10}Be ground state. From Eq. (3) one then deduces the corresponding "experimental" photopion results and these are represented by the data points in Fig. 6.

The solid curve in Fig. 6 was calculated by combining Eqs. (3) and (7), yielding

$$\left[\frac{d\sigma}{d\Omega_\pi}\right]_\gamma = 8.35\times10^{-3}Z^2 \times\frac{p_\pi}{k_\gamma}C_0^2(\eta)\chi(\theta_\pi,\theta_q)\left[\frac{F_{M\lambda}^2(q)}{q^2}\right], \quad (10)$$

where as before $F_{M\lambda}^2(q)$ was obtained from a Helm model fit to the 1.74 MeV form factor.[3] Since this fit does not take into account the Coulomb distortion effects in the electron scattering data, we have refitted those data using the effective-q approximation, in which the experimental q values are replaced by

$$q_{\text{eff}} = q\left[1+\frac{3\alpha Z}{2E_eR}\right],$$

where E_e is the incident electron energy and $R=(\frac{5}{3})^{1/2}r_{\text{rms}}$ is the radius of the equivalent sphere. The resulting (γ,π^+) cross section is the dashed curve in Fig. 6. The two curves differ by 10–20%, and although the effective-q approximation tends to exaggerate the Coulomb corrections, it does suggest that such effects are not negligible.

Finally, in Fig. 7 we compare the $\theta_\pi=90°$ cross sections given by Eq. (10) with the recent work of Rowley *et al.*[11] and Bosted *et al.*[12] Actually, the energy region of the latter authors extends far beyond the range where the present simple model has much validity, so the favorable comparison evident in Fig. 7 at high pion energies is somewhat puzzling.

A more complete treatment of the photoproduction and electroproduction cross sections would entail full distortion of the pion wave function by the strong and Coulomb forces, and would require knowledge of the nuclear transition spin

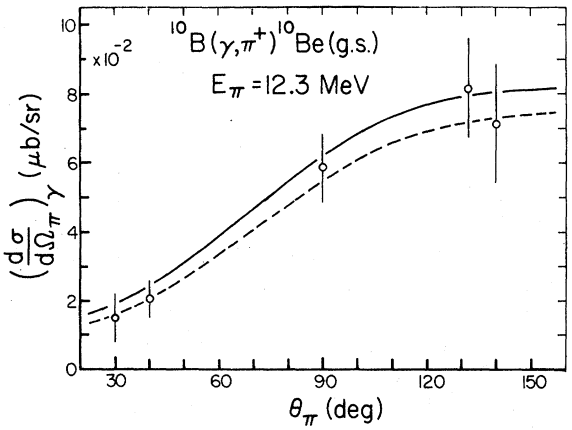

FIG. 6. Photopion angular distribution leading to the ^{10}Be ground state as deduced from the data in Fig. 2. The solid curve is based on the $M3$ form factor for the 1.74 MeV state of ^{10}B. For the dashed curve some allowance was made for Coulomb distortion of the (e,e') data by using the effective-q approximation.

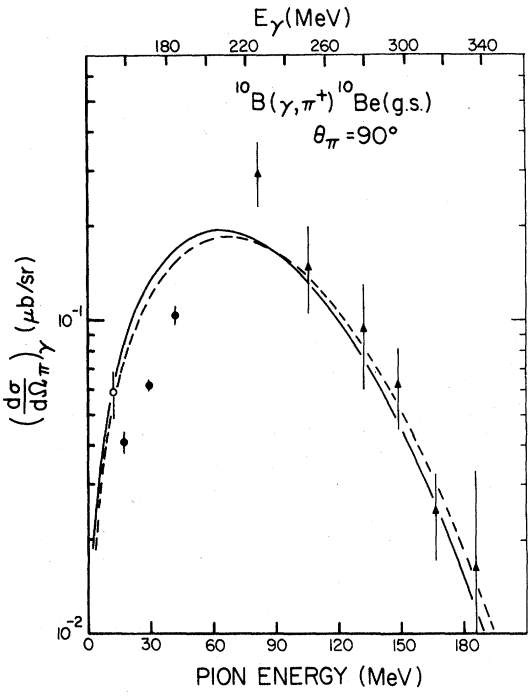

FIG. 7. The 90° photopion cross section leading to the ^{10}Be ground state, as a function of the pion kinetic energy. The open-circle point is from this work, the closed-circle points are from Rowley *et al.* (Ref. 11), and the triangle points are from Bosted *et al.* (Ref. 12). The curves are as in Fig. 6.

densities. For stretched $M\lambda$ transitions these densities can be obtained directly from the form factors by Fourier-Bessel analyses, for example, but in any case are relatively model independent. Thus, the low lying $M3$ transitions appear to be good candidates for exploring the final state π-nucleus interaction where assumptions concerning the structure of the participating states must be kept to a minimum.

ACKNOWLEDGMENTS

The authors wish to thank Prof. E. L. Tomusiak for helpful discussions. This work was supported by a grant from the Natural Sciences and Engineering Research Council of Canada.

[1]J. C. Bergstrom, Phys. Rev. C 21, 2496 (1980).
[2]P. Truöl, *Proceedings of the International Conference on Nuclear Physics with Electromagnetic Interactions, Mainz, 1979,* edited by H. Arenhövel and D. Drechsel (Springer, Berlin, 1979).
[3]E. J. Ansaldo, J. C. Bergstrom, R. Yen, and H. S. Caplan, Nucl. Phys. A322, 237 (1979).
[4]R. M. Sealock, H. S. Caplan, M. K. Leung, G. J. Lolos, and S. Hontzeas, Nucl. Instrum. Methods 157, 29 (1978).
[5]P. Stoler *et al.*, Phys. Rev. C 22, 911 (1980).
[6]E. Borie, H. Chandra, and D. Drechsel, Nucl. Phys. A226, 58 (1974).
[7]W. C. Haxton, Nucl. Phys. A306, 429 (1978).
[8]R. H. Dalitz and D. R. Yennie, Phys. Rev. 105, 1598 (1957).
[9]S. Furui, Prog. Theor. Phys. 58, 864 (1977).
[10]A. Nagl and H. Überall, Phys. Lett. 96B, 254 (1980).
[11]D. Rowley *et al.*, Phys. Rev. C 25, 2652 (1982).
[12]P. E. Bosted, K. I. Blomqvist, A. M. Bernstein, S. A. Dytman, and R. A. Miskimen, Phys. Rev. Lett. 45, 1544 (1980).